

Multi-Channel Microring Weight Bank Control for Reconfigurable Analog Photonic Networks

Alexander N. Tait, Allie X. Wu, Ellen Zhou, Thomas Ferreira de Lima,
Mitchell A. Nahmias, Bhavin J. Shastri, and Paul R. Prucnal
Princeton University, Princeton, NJ, 08544 USA
atait@princeton.edu

Abstract—We demonstrate 4-channel weighted addition in a silicon microring filter bank with 3.8 bit accuracy. Scalable calibration techniques are developed for thermal cross-talk and cross-gain saturation. Practical weight control is essential for large-scale photonic processing based on microrings.

I. INTRODUCTION

The memory-processor bottleneck inherent in conventional computers has recently inflamed two global research thrusts: 1) integrated photonics manufacturing, in which the aim is to address this bottleneck's performance, and 2) unconventional computing architectures, in which the aim is to eliminate it altogether. Unconventional architectures in electronics are distributed, thereby relying heavily on multi-access networking strategies. Much recent work has focused on neuron-inspired models, in which network connections are represented by programmable real number “weights” [1]. The intersection of these two fields could yield cost-effective processors with unprecedented speed and complexity.

Optical approaches to the analog/neural interconnect problem have long been recognized, but so far none have been integrated. A silicon photonic analog networking approach called “broadcast-and-weight” (Fig. 1a) was proposed in [2]. Weighted connections are implemented by tunable microring resonator (MRR) weight banks (Fig. 1b). MRR circuits have the advantages of compactness, WDM capability, and ease of tuning. On the other hand, MRR sensitivity to fabrication variations, thermal fluctuations, and thermal cross-talk presents a control problem. The unique requirements of a MRR weight bank call for a feedforward control approach with offline pre-calibration performed at least once per fabricated device [3]. When weight interdependency is present, the dimensionality of the full tuning range increases with N , necessitating $O(2^N)$ calibration measurements in the naive case.

We show for the first time simultaneous multi-channel weight control whose calibration time scales linearly with channel count, $O(N)$. The 4-channel bank attains a weight accuracy of 3.8 bits, plus 1.0 sign bit (i.e. 28 distinguishable weights from -1 to $+1$). Model-based calibration techniques are introduced to deal with predominant sources of weight interdependency: thermal cross-talk and cross-gain saturation. This weight resolution matches state-of-the-art electronic counterparts [1]. Practical, accurate, and scalable MRR control techniques are a critical step towards large scale analog processing networks based on MRR weight banks.

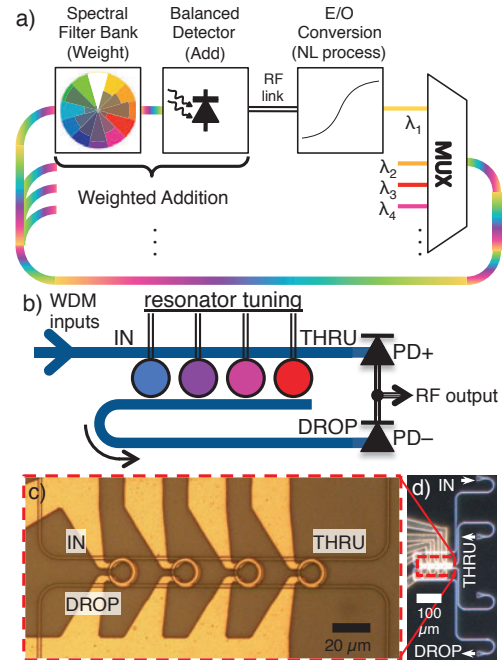


Fig. 1. a) On-chip analog processing network, from [2]. Weighted addition banks drive E/O converters, each using a distinct wavelength. b) Microring resonator (MRR) implementation of a WDM weight bank. Continuous tuning between on- and off-resonance directs power between DROP and THRU ports. A balanced photodetector (PD) yields the sum and difference signals. c-d) Micrographs of a 4-channel tunable MRR weight bank under test.

Samples were fabricated on 220nm thick silicon-on-insulator wafers through UBC SiEPIC [4]; waveguides are fully-etched, 500nm wide, and oxide-clad. Ti/Pt/Au heating contacts were then deposited to provide thermo-optic MRR resonance tuning. The sample is mounted on a temperature-controlled alignment stage and coupled to fiber with focusing subwavelength grating couplers [4]. The weight bank device consists of two bus waveguides and four MRRs in a parallel add/drop configuration (Fig. 1c). Each MRR controls a single WDM channel by tuning continuously on- or off-resonance. The experimental setup (Fig. 2a) consists of an input generator that produces statistically independent references by imparting channel-dependent delays on a 2Gbps pseudo-random bit sequence (PRBS) (Fig. 2b). The effective weight vector

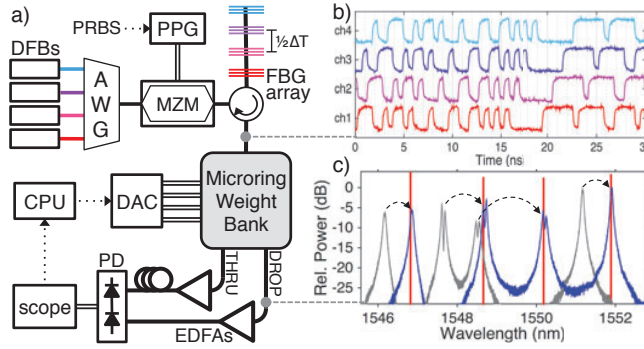


Fig. 2. a) Experimental setup. An input generator creates four signals on different wavelengths, traces shown in (b). DFB: distributed feedback laser; AWG: arrayed-waveguide grating; PPG: pulse pattern generator; MZM: Mach-Zehnder Modulator; FBG: fiber Bragg grating. The microring weight bank is thermally tuned by a 13-bit current-mode DAC (digital-to-analog converter). The DROP and THRU outputs of the MRR weight bank are amplified, their net delays matched, and detected by a balanced photodiode (PD). A CPU controls the calibration routine. c) Optical spectrum of input WDM signals (red) and DROP port when tuning current is off (gray) and biased onto resonance (blue).

is determined by projecting the measured output onto this reference basis. The calibration routine performed by a CPU estimates a mapping of applied current to weight $\vec{i} \rightarrow \vec{\mu}$. The inverse of this mapping becomes the feedforward control rule.

Thermal cross-talk occurs when heat leaks from a given heater to a neighboring MRR. While the heat transfer effect is linear in dissipated electrical power, heater resistance can also change with temperature. This thermo-electric contribution results in slight nonlinearity in current-squared, which can be incorporated into a multivariate Taylor approximation.

$$\vec{\lambda} - \lambda_{res} \approx \sum_{d=1}^D \mathbf{K}_d \left(\vec{i}^2 - i_{res}^2 \right)^d \quad (1)$$

where $\vec{\lambda}_{res}$ are WDM wavelengths, i_{res} are bias currents on-resonance, D is Taylor order, and \mathbf{K}_d is the d^{th} -order coefficient matrix. $D = 1$ is equivalent to a constant-resistance approximation. Once \mathbf{K} coefficients are fit, the model can be inverted iteratively to obtain the control rule. The transmission effect of each MRR filter edge is then calibrated with an interpolation-based approach originally developed for a single channel [3]. A relatively large channel spacing (Fig. 2c) ensures that optical cross-talk can be neglected. EDFAs at the output of the weight bank (Fig. 2a) are subject to cross-gain saturation, which depends on the bank's transmission vector. We develop a parameterized model for cross-gain saturation effects (details omitted for space). Much like the parameterized thermal model, it can be calibrated in linear time and the model inverted to yield a control rule.

After the calibration procedure is performed, the command weight is swept in two-dimensions at a time while the actual weight is measured (Fig. 3). Other pairs of channels (not plotted) were seen to produce similar results. Errors can be quantified in terms of accuracy, a.k.a. mean error (red lines), and precision, a.k.a. dynamic error (blue ellipses). Mean

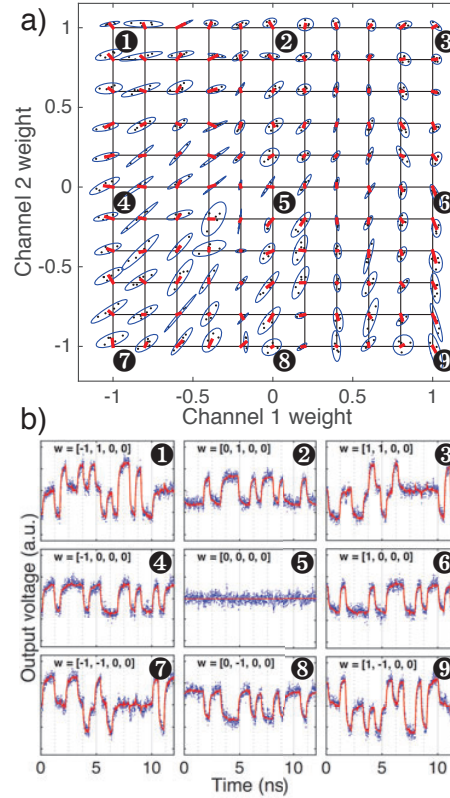


Fig. 3. a) Two-dimensional weight sweep analyzing controller accuracy and precision. After a calibration procedure with $D = 2$ thermal model, the target weight is swept 5 times from -1 to $+1$ (black grid). Black points are measured weights. Red lines indicate mean offset from target grid points. Blue ellipses indicate one standard deviation around the mean. b) Output traces (identical axes) corresponding to points labeled in (a). Red: expected, blue: measured.

error is less than 0.072 over the range (3.8 bit accuracy), and dynamic standard deviation is less than 0.062 (4.0 bit precision). DAC resolution (13 bits) is expected to limit mean error due to extreme sensitivity enhancement, such as filter sharpness. Filter sharpness can not be reduced; however, large required bias currents (~ 50 mA) also significantly enhance sensitivity. MRRs designed to have lower bias currents are thus expected to improve accuracy by several bits.

Control strategies will be a crucial component of large-scale MRR systems, particularly in the analog case. We introduced a scalable modelling approach for thermal effects (incl. thermo-electric) and cross-gain saturation, showing 4-channel control with 3.8 bit accuracy. Further work could explore the channel density limits and the integration of multiple weight banks into a broadcast-and-weight network.

REFERENCES

- [1] F. Akopyan *et al.*, *Computer-Aided Design of Integrated Circuits and Systems, IEEE Transactions on*, vol. 34, no. 10, pp. 1537–1557, Oct 2015.
- [2] A. N. Tait *et al.*, *J. Lightwave Technol.*, vol. 32, no. 21, pp. 3427–3439, Nov 2014.
- [3] A. Tait *et al.*, *Photonics Technology Letters, IEEE*, no. 99, pp. 1–4, 2016.
- [4] Y. Wang *et al.*, *Optics express*, vol. 22, no. 17, pp. 20652–20662, 2014.